https://dx.doi.org/10.1016/j.buildenv.2021.108586

Effectiveness of Personalized Air Curtain in Reducing Exposure to Airborne Cough Droplets

Jingcui Xu, Hai Guo*, Yanling Zhang, Xiaopu Lyu

Air Quality Studies, Department of Civil and Environmental Engineering, The Hong Kong Polytechnic University, Hong Kong, China

Correspondence email: ceguohai@polyu.edu.hk

Abstract

To minimize infection risk of airborne transmission during close contact, a personalized air curtain (PAC) system was proposed to protect users from airborne droplets. This work investigated the performance of PAC in reducing exposure to airborne droplets through two thermal manikins in close proximity (0.82 m). A cough generator was put into one of the manikins (an infected person) to release cough droplets to simulate coughing activities. Concentration of airborne droplets in the inhalation zone of the other manikin, as a healthy person (HP), was measured. The effect of PAC with different flow rates (from 9 L/s to 27 L/s) and distances to the HP (15 cm to 65 cm) on exposure to airborne droplets was investigated. The performance of PAC was further compared with that of personalized ventilation (PV), integrated PAC-PV, and partitions. Visualization experiments were performed to observe the interaction between the cough jet and PAC, PV, PAC-PV, and partitions. The results showed that exposure reduction caused by PAC was from 42% to 87% considering the flow rate and distance between HP and PAC. When the PAC velocity increased to 'critical velocity', *i.e.*, 5 m/s, the exposure reduction was nearly stable and the distance between PAC and HP has almost no influence on the exposure reduction. Besides, exposure reduction of integrated PAC-PV was between 94% and 98%, showing a quite

good performance in reducing airborne droplets. The results indicated that PAC and PAC-PV could be used as mitigation measures to protect users and reduce exposure to airborne droplets.

Keywords: Respiratory disease transmission; Airborne droplet; Personalized air curtain; Exposure reduction; Mitigation measure

1 Introduction

The outbreaks of epidemic respiratory diseases worldwide such as COVID-19, influenza, and severe acute respiratory syndrome (SARS), cause high human morbidity and mortality, and threaten human safety and living standards. Studies show that human expiratory activities such as breathing, talking, coughing and sneezing from infected people, are the major source of respiratory disease transmission [1-3] since numerous pathogen-laden droplets are released from these expiratory activities. Sufficient evidence has demonstrated that the transmission of respiratory diseases has a strong association with ventilation and air movements in indoor environments [4, 5]. Expiratory droplets (< 10 μm in diameter) can be dispersed widely in indoor environments and inhaled by exposed people [6]. Exposure to airborne pathogen-laden droplets is likely to result in airborne infection. As people spend increasing time in indoor environments, the issue of inhaled air quality has attracted more and more attention.

Hence, to reduce the airborne transmission of respiratory infection in indoor environments, different ventilation strategies have been proposed in the past. For instance, to better alleviate airborne infection risk, increasing flow rates of total volume ventilation was suggested [4, 7]. An increase of ventilation rate indoors usually lowers

pathogen concentration and reduces airborne infection risks [8-10]. However, increasing the overall ventilation rate substantially results in heavy energy consumption. Even more, some studies reported that a higher ventilation rate could possibly cause an increased exposure to exhaled droplets. Bolashikov et al. [11] found that a ventilation rate of 12 h^{-1} resulted in a higher exposure of doctors compared to ventilation rates of 3 and 6 h^{-1}. Pantelic et al. [12] also presented similar findings. Therefore, the ventilation rate should not be used as the only indicator of the performance of the ventilation systems. Instead, the local airflow patterns around people should be emphasized.

Recent studies revealed that personalized ventilation (PV) was a good control measure to reduce and prevent airborne infections [13-15]. Xu et al. [16, 17] found that PV effectively reduced the exposure of users to airborne droplets, and the reduction of bioaerosol inhalation was between 52% and 100% depending on the PV velocity and the distance between the infected person and the healthy person. Li et al. [18] and Shen et al. [19] indicated that PV flow could reduce the exposure to exhaled droplet nuclei, while the effectiveness of PV flow was highly related to the background ventilation system, and the types of PV terminals played an important role in the performance of PV flow. Yang et al. [20] investigated a novel PV-PE (personalized exhaust) system as a tool for airborne infection control, and concluded that the combined PV-PE system could achieve the lowest intake fraction of the air exhaled by an infected person. Pantelic et al. [21, 22] revealed that PV reduced the intake fraction of cough droplets by 41% to 99% depending on the distance and orientations of the cough jet. However, PV could also result in higher exposure in some cases. When PV is used only by infected persons, healthy people have an increased risk of infection, compared with using total volume ventilation alone [18, 23, 24]. All these studies highlighted that PV could improve the microenvironmental air quality in most cases and the use of PV only

by infected people should be avoided. Nevertheless, the high velocity of the PV airflow was used to offset the expiratory droplet velocity and protect the users, while the airflow velocity around the face might cause draught sensation and eye dryness.

Apart from PV, a protected occupied zone ventilation (POV) system was proposed to reduce the airborne cross-infection [25]. The protection efficiency of POV to exhalation was from 8% to 50% depending on the exhaust location, supply air velocity and usage of partitions [25]. Cao et al. [26] investigated the protection of POV with two standing manikins during close contact from 0.35 m to 1.1 m. They found that personal exposure was reduced by POV up to twenty times lower than that by displacement ventilation and downward airflow ventilation. Aganovic et al. [27] reported that the POV ventilation strategy to protect medical staff in the hospital isolation wards was effective. These studies show that the downward plane airflow of the POV can bend the exhaled airflow towards the lower part of the exposed people and divide an indoor space into subzones: source zone and target zone. Since exhalation does not penetrate the plane jet, protection can be guaranteed. There are, however, some concerns about the application of POV. The flexibility of POV in space use is limited. Once the system is installed, it is difficult to relocate air diffusers. Furthermore, draught risk is a problem with POV [28].

To better improve the inhaled air quality and solve the aforementioned problems, we propose a personalized air curtain (PAC) system to reduce the risk of exposure to airborne transmission during close contact. The PAC system blows up vertically and can be installed on a table or desk. The high velocity of the airflow may block or change the direction of movement of incoming expiratory droplets. So far, we have not been very clear about the protection of the PAC system in the case of close contact.

This study aims to investigate the effectiveness of the PAC system in reducing

the airborne infection risk through experiments. Specifically, the performance of PAC with different flow rates and different distances from healthy people in mitigating exposure to airborne droplets is studied. In addition, we compare the effectiveness of PAC with that of PV, integrated PAC-PV, and partitions that are now widely used due to COVID-19.

2 Methodology

2.1 Experimental design

The experiments were performed in a chamber with a dimension of 2.4 m (width) × 3.2 m (length) × 2.9 m (height) equipped with a mixing ventilation system, as shown in Fig. 1. During the experiments, the temperature and relative humidity were maintained at 23.5 ± 0.5 ^{o}C and 65 ± 3 %, respectively. The air change rate of the mixing ventilation system was 5.0 h^{-1}, which was measured by the method of tracer gas (CO_2) concentration decay.

Two thermal manikins used in a previous study [17] with a sitting height of 1.4 m and clothing insulation of 0.46 clo were used to mimic an infected person (IP) and a healthy person (HP). To simulate a moderate office work, the heat release of the IP and HP was set to 70 W [29]. The distance between the IP and HP in this work was 82 cm, which meant that two people were in close contact. Such a case might occur when two people have face-to-face conversations, such as doctor-patient interactions in hospitals, discussion in offices and conversations in public transport (e.g. trains and buses).

Simulated saliva solution was prepared by dissolving 76 g glycerin and 12 g salt (NaCl) in 1 L distilled water [30]. A cough generator with a nozzle was used to generate cough droplets. The detailed information of the cough generator can be found in previous studies [17, 30]. The nozzle was put into the mouth of the IP. The equivalent diameter of the nozzle was around 15 mm, as shown in Fig. 1S. The releasing velocity

of cough jet was about 12 m/s. Cough droplets were generated horizontally from the nozzle in this work. In each measurement, the cough release lasted for 1 s three times with an interval of 5 s.

The concentration of airborne cough droplets in the inhalation zone of the HP was measured by an optical particle sizer (OPS) (Model 3330, TSI, Shoreview, MN, USA) and a corresponding dilutor (Model 3332, TSI, Shoreview, MN, USA). The concentrations of droplets with sizes from 0.3 μm to 10 μm were measured at an interval of one second. The sampling rate was 1 L/min. For each measurement, the total measurement time was 11 min. One minute was used to measure the background concentration before the cough release. The average concentration of this one-minute measurement was used as the background concentration for the following calculation. The other ten minutes were used for the measurement after the release. The concentration of airborne droplets could decay to the background concentration level within the 10 minutes.

2.1.1 Personalized air curtain

A personalized air curtain (PAC) system was used to blow the air vertically upward between the HP and the IP. The outlet size of the PAC terminal was 30 cm × 1 cm. During the experiments, the horizontal distance between the HP and the PAC terminal was 15 cm, 40 cm, and 65 cm, as shown in Fig. 1 (b). The vertical distance from PAC outlet to the inhalation zone was 30 cm. The flow rate of the PAC was set to 9, 15, 21 and 27 L/s, respectively. The corresponding velocity at PAC outlet was 3.0, 5.0, 7.0, and 9.0 m/s, respectively. The velocity was measured by a hotwire anemometer (Model 9535, TSI, Shoreview, MN, USA). The velocity range of the hotwire anemometer is 0 - 30.0 m/s with an accuracy error of ±3% and a resolution of 0.01 m/s. The noise increased within 3 dB when the PAC airflow was at a velocity of 3, 5, 7, and

9 m/s.

The PAC system was installed inside the test chamber. The system was supplied with recirculated room air, which was filtered by a HEPA filter (H13 filter, PM0.3, 99.97%) in the air duct of the PAC. The recirculated and filtered room air was used to supply PAC instead of clean air externally, which was helpful to keep the integrity of the chamber and simplify the experimental setup.

It should be noted that the PAC in this study was different from the vertical desk grills (VDG) and horizontal desk grills (HDG) of different types of personalized ventilation terminals in the previous studies [19, 31-33], which faced the users directly. VDG and HDG supplied a slanted upward jet of clean air to the user's inhalation zone and toward the user's body, respectively. Differently, PAC in this study vertically sent the airflow upward between the healthy person and infected person, as shown in Fig. 1 (c).

2.1.2 Personalized ventilation

A personalized ventilation (PV) system was used to compare the performance of PAC and PV. The circular PV terminal had a diameter of 0.108 m with a honeycomb flow straightener. The distance between the centre of the PV outlet and the HP's inhalation zone was 30 cm. The angle between the horizontal line and the normal line of the PV terminal was 80^{o}, as shown in Fig. 1 (a). The location of PV was fixed in this study. In order to compare the performance of PAC with PV, the flow rate of PV was also set to be 9, 15, 21 and 27 L/s. Similar to PAC, the PV system was also installed inside the test chamber. The same type of HEPA filter applied in PAC was used.

2.1.3 Partition

Partitions with two different widths of 30 cm and 68 cm were investigated. The width of 30 cm was the same as PAC. The width of 68 cm was the same as the table

used in this work. The height was 51 cm, 23 cm higher than the inhalation zone of the HP in vertical distance. The partition was placed at 15, 40, and 65 cm from the HP, the same distance as the PAC.

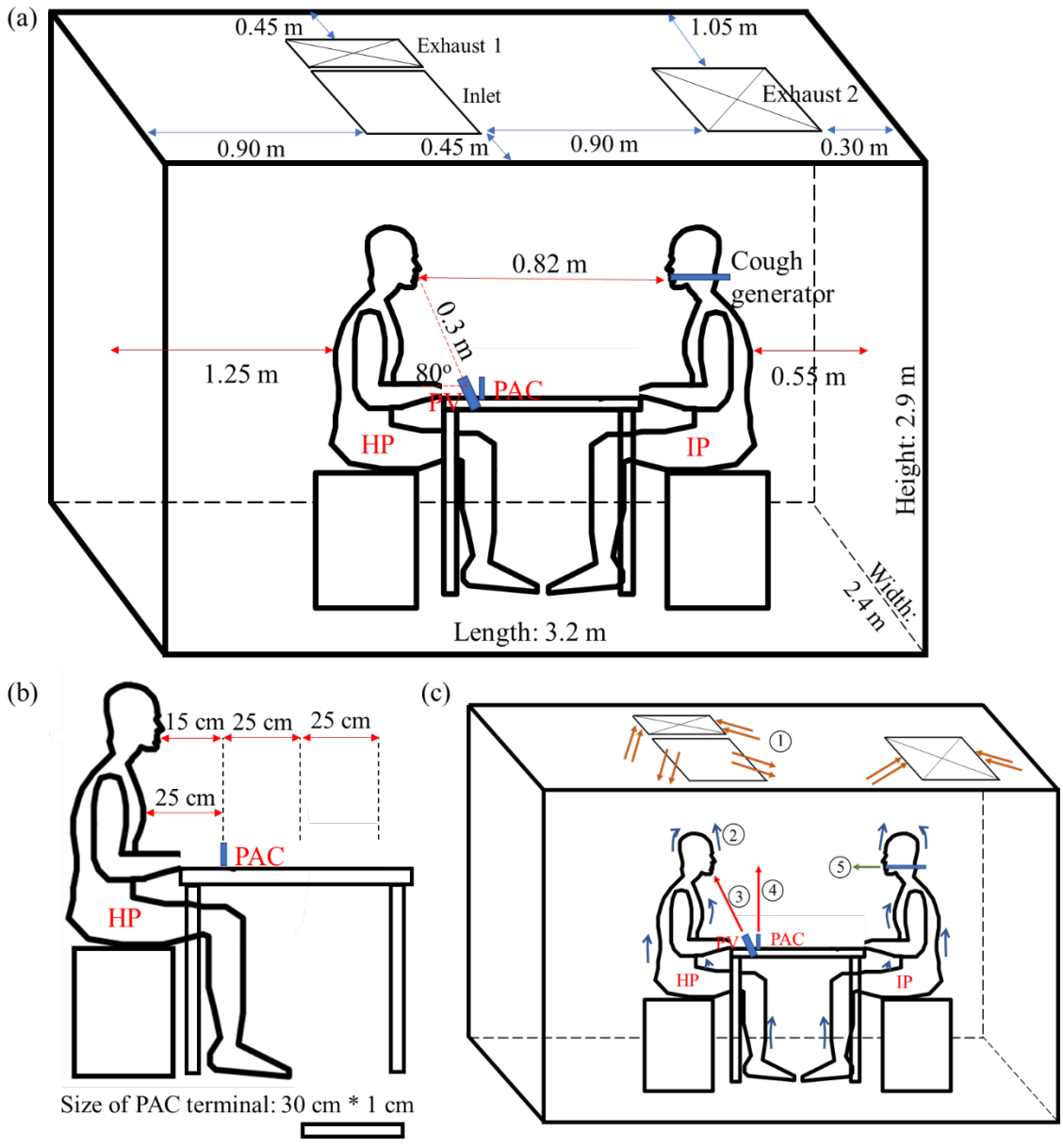

Fig. 1 (a) Configuration of the experimental setup in the chamber. The size of inlet, exhaust 1 and exhaust 2 of the background ventilation system is 0.45 m × 0.90 m, 0.45 m × 0.45 m, and 0.45 m × 0.90 m, respectively. (b) Locations of personalized air curtain (PAC). (c) Main air flows in the chamber. 1. background ventilation flow; 2. free

convection flow; 3. airflow from PV; 4. airflow from PAC; 5 cough jet from the IP.

2.2 Experimental scenarios

The experimental scenarios are shown in Table 1. This study first investigated the performance of PAC with different flow rates (*i.e.* 9, 15, 21 and 27 L/s) and at different distances from the HP (15, 40 and 65 cm) in reducing the concentrations of airborne droplets. Then, the effectiveness of PV with flow rates of 9, 15, 21 and 27 L/s was assessed. Furthermore, the performance of the integrated PAC-PV and partitions was measured. Each experiment in this work was repeated three times.

Table 1 The details of experimental scenarios

Measurement condition	Scenario	PAC jet supply Velocity (m/s)
Background ventilation	Mixing ventilation	N/A
PAC	PAC/9-D15[a]	3.0
	PAC/9-D40	3.0
	PAC/9-D65	3.0
	PAC/15-D15	5.0
	PAC/15-D40	5.0
	PAC/15-D65	5.0
	PAC/21-D15	7.0
	PAC/21-D40	7.0
	PAC/21-D65	7.0
	PAC/27-D15	9.0

	PAC/27-D40	9.0
	PAC/27-D65	9.0
PV	PV/9[b]	N/A
	PV/15	N/A
	PV/21	N/A
	PV/27	N/A
Integrated PAC-PV	PAC/9+PV/12-D15[c]	3.0
	PAC/9+PV/12-D40	3.0
	PAC/9+PV/12-D65	3.0
	PAC/9+PV/18-D15	3.0
	PAC/9+PV/18-D40	3.0
	PAC/9+PV/18-D65	3.0
Partition	P(30)-D15[d]	N/A
	P(30)-D40	N/A
	P(30)-D65	N/A
	P(68)-D15	N/A
	P(68)-D40	N/A
	P(68)-D65	N/A

[a] PAC/9-D15 means that the flow rate of the PAC is 9 L/s and the distance between the PAC and the HP is 15 cm.

[b] PV/9 denotes that the flow rate of the PV is 9 L/s. The location of the PV is fixed.

[c] PAC/9+PV/12-D15 represents that the flow rate of the PAC is 9 L/s and the flow rate of the PV is 12 L/s. The total flow rate is 21 L/s. D15 means that the distance between the PAC and the HP is 15 cm.

[d] P(30)-D15 indicates that the width of the partition is 30 cm. The distance between the partition

and the HP is 15 cm.

To evaluate the performance of PAC, PV, integrated PAC-PV and partitions, their exposure reduction was calculated using the following equation (1) [20].

$$\varepsilon = \frac{C_{off} - C_{on}}{C_{off}} \quad (1)$$

where, C_{off} is the average concentration of airborne droplets in the inhalation zone when there is no protection system (*i.e.* PAC, PV, PAC-PV and partition). C_{on} is the average concentration of airborne droplets in the inhalation zone when PAC or PV or PAC-PV or partition is in operation. When C_{on} is smaller, the exposure reduction is higher. The higher the exposure reduction is, the better the air quality is. In the calculation, the average background concentration was subtracted from the real-time concentration after cough release.

2.3 Visualization experiments

To visually observe the interaction between cough jet and PAC or PV or integrated PAC-PV or partition, experiments were designed, as shown in Fig. 2. Two LED lights were used as the light source. The power for LED lights was 40 W. A camera was applied to record the interaction for visualization. The LED was 'cool light', thus the temperature around the LED was almost not increased when the LED was turned on. The surface temperature of the light barrier was increased within 0.2 ºC during the visualization experiment. Hence it is reasonable to assume that the LED light had tiny influence on the interaction between the cough jet and PAC or PV or integrated PAC-PV or partition.

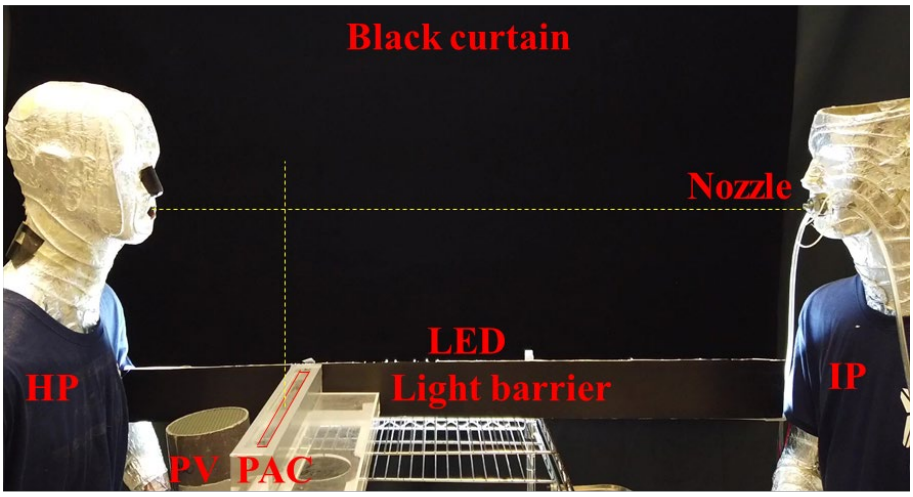

Figure 2 Setup for visualization experiments

3 Results

3.1 Velocity distribution

The centre velocity distribution starting from the outlet of PAC was measured when the PAC had a flow rate of 9, 15, 21 and 27 L/s, respectively, corresponding to a supply velocity of 3.0, 5.0, 7.0, and 9.0 m/s, respectively (Fig. 3 (a)). The vertical velocity, at the cross point of horizontal cough jet and vertical PAC flow (red dot line at 30 cm height in Fig. 3 (a)) was about 1.2, 1.9, 2.6 and 3.2 m/s, respectively. When the height increased to 60 cm from the PAC outlet, the vertical velocity decayed to 0.9, 1.3, 1.7 and 2.1 m/s, respectively. Furthermore, when the PV had a flow rate of 9, 15, 21 and 27 L/s, the PV centreline velocity in the HP's inhalation zone was approximately 0.9, 1.5, 2.0 and 2.5 m/s, respectively, as shown in Table 2.

Table 2 Centreline velocity in the inhalation zone of the HP of the PV with different flow rates

Scenario	PV/9	PV/15	PV/21	PV/27
Velocity in inhalation zone (m/s)	0.9	1.5	2.0	2.5

For the PAC airflow, the decay of the centreline velocity of a plane jet in the developed region was calculated using the following equation (2)

$$U_y/U_0 = K/\sqrt{y/h} \quad (2)$$

The meaning of each parameter in Eq. (2) is listed in Table 3. A value of 2.4 of K was used in this work to calculate the decay of centreline velocity based on the recommendation from previous studies [34, 35]. h was one centimetre in this study. Fig. 3 (b) presents the dimensionless decay of the centreline velocity of the PAC along the distance upstream from the centre line of PAC. The dimensionless velocity decay profile indicated that PAC flow behaved like a plane jet.

Table 3 Meaning of each parameter in Eq. (2)

U_y (m/s)	Centreline velocity at a distance of y (m) upstream from the PAC terminal
U_0 (m/s)	Supply velocity
K	Dimensionless constant of the jet
y	Distance upstream from the PAC
h	Width of PAC

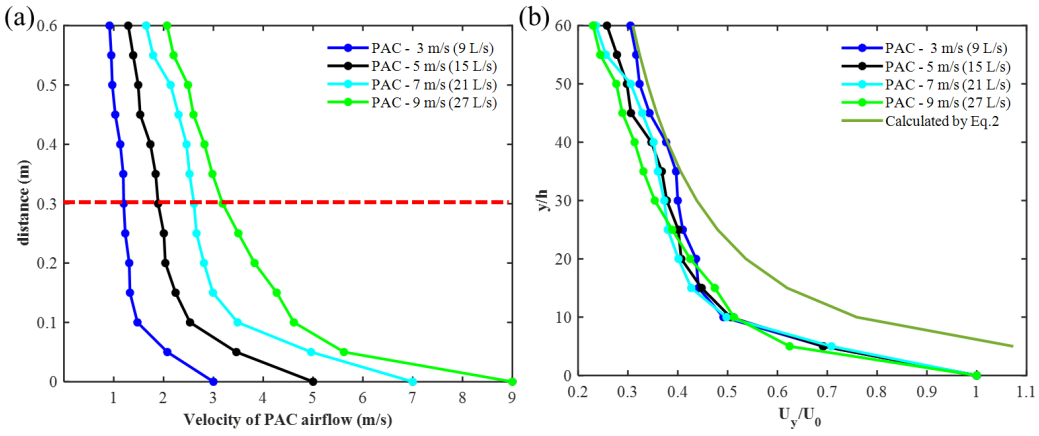

Figure 3 (a) Vertical profile of average velocity with the PAC on. The red dot line

represents the height of the inhalation zone from the PAC outlet. (b) Dimensionless decay of the centreline velocity of the PAC

3.2 Performance of PAC

This work focused on the airborne droplets with diameters of 0.3-10 μm in the HP's inhalation zone. The cough release lasted for one second each time. From the visualization of the case where there was only background ventilation system (Fig. 2S), we can see that the cough jet moved directly to the HP and the cough jet reached the HP in 0.6 s after release. Wei et al. [36] indicated that droplet nuclei less than 10 μm would follow the cough jet within a distance of 1 m from the release point. The cough jet around the HP observed in Fig. 2S implied that the airborne droplets (0.3-10 μm in diameter) surrounded the HP.

Fig. 4 shows the motion of cough jet when PAC had a supply velocity of 3 m/s at a distance of 15 cm from the HP. Compared to the case only with the background ventilation system, PAC flow with a velocity of 3 m/s somewhat changed the motion of cough droplets, but some droplets still penetrated the PAC flow and entered the inhalation zone. When the velocity of PAC was increased to 5 m/s (Fig. 3S), 7 m/s (Fig. 4S) and 9 m/s (Fig. 5) at 15 cm from the HP, the cough jet was blocked by the PAC flow and could not pass through the PAC flow. The PAC flow acted as a 'barrier' to deflect the cough jet, which was different from the PAC flow at a velocity of 3 m/s (Fig. 4).

In comparison, PAC with a velocity of 3.0 m/s could not effectively prevent the cough droplets from moving to the HP, while a PAC with a velocity of 5.0 m/s or higher was able to block the cough jet.

Figure 4 Visualization of interaction between the cough jet and the PAC-generated air jet for the case of PAC with a supply velocity of 3 m/s or a flow rate of 9 L/s. The distance between the PAC and the HP is 15 cm. t = 0 s means the start of cough release; t = 1 s means the end of cough release.

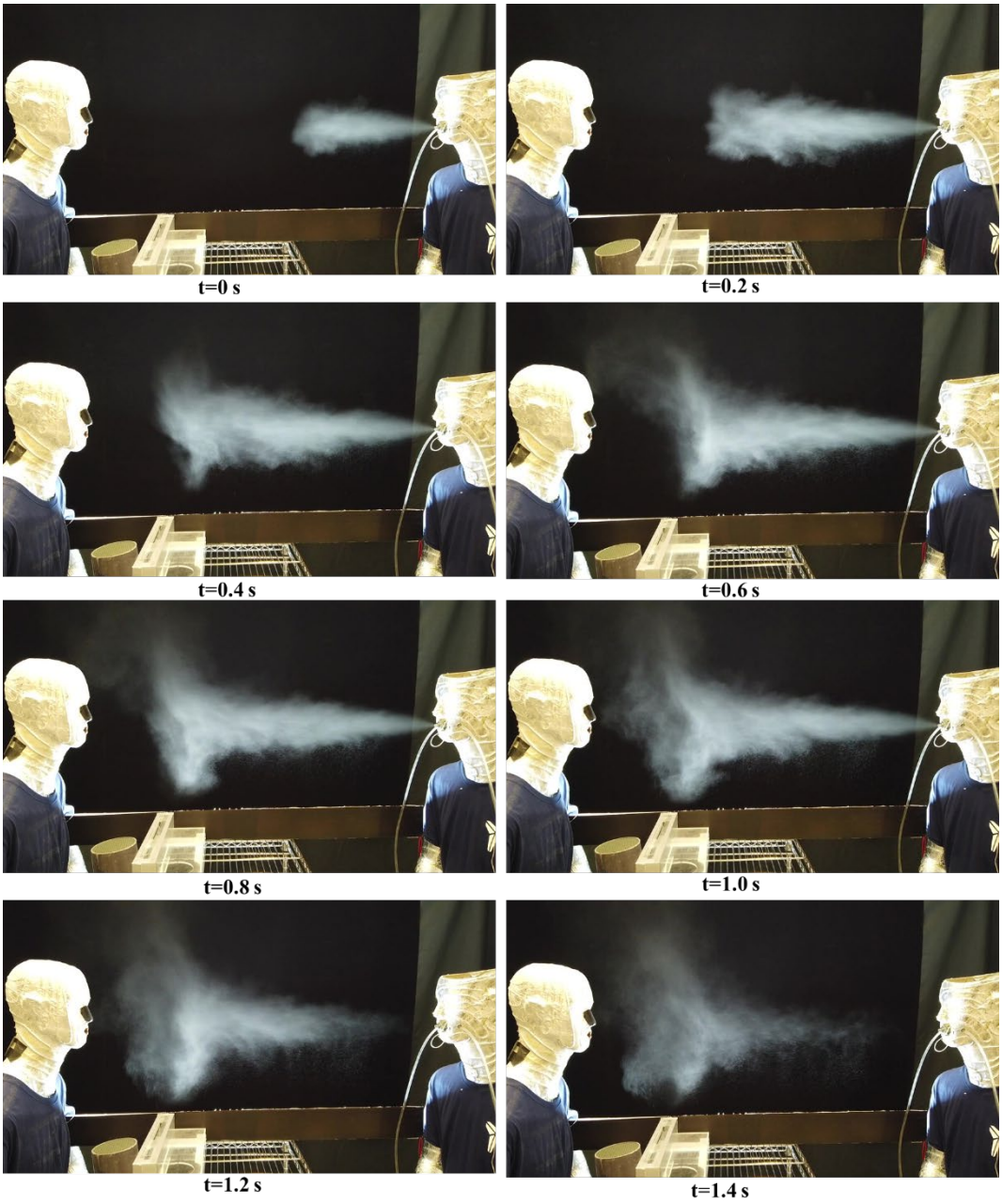

Figure 5 Visualization of interaction between the cough jet and the PAC-generated air jet for the case of PAC with a supply velocity of 9 m/s or a flow rate of 27 L/s. The distance between the PAC and the HP is 15 cm.

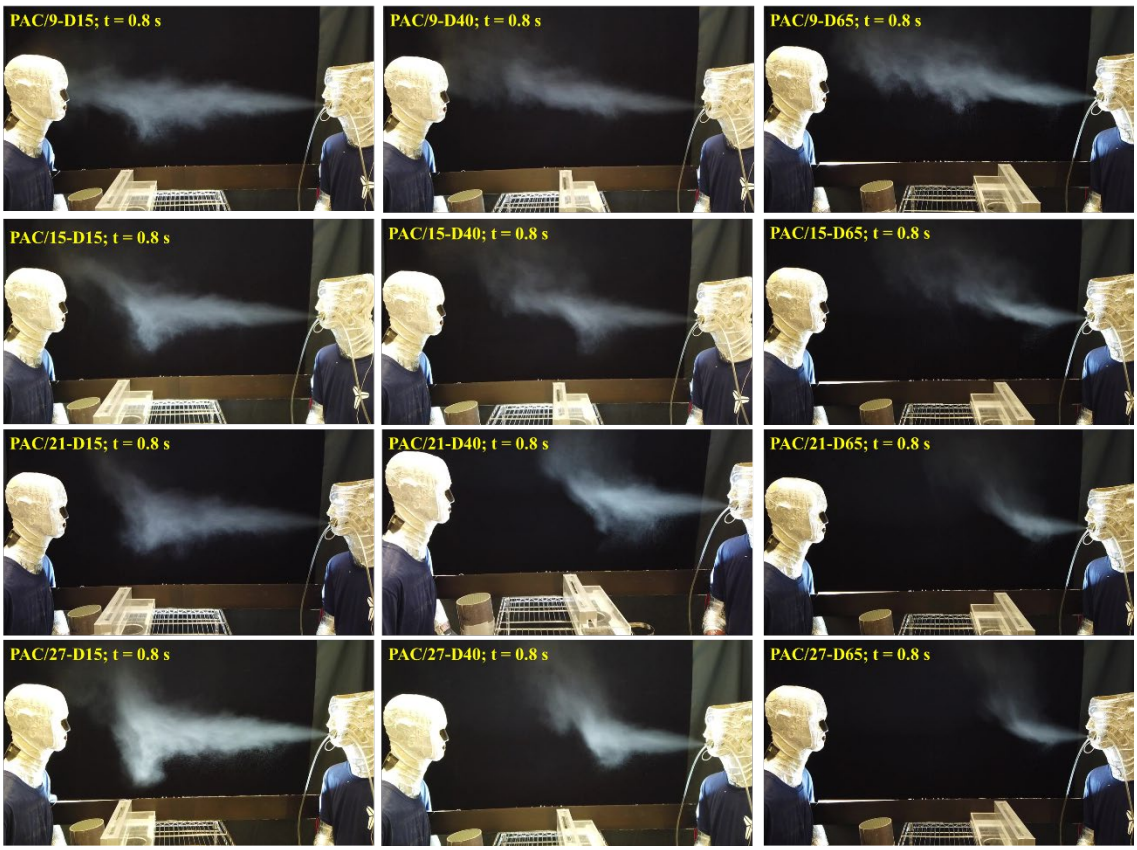

Figure 6 Visualization of interaction between the cough jet and the PAC-generated air jet at t = 0.8 s. The distance between the PAC and the HP is 15, 40, and 65 cm. The flow rate of the PAC is from 9 to 27 L/s. The PAC supply velocity is from 3 to 9 m/s.

Fig. 6 shows the impacts of the PAC with different supply velocities at different distances from the HP on the interaction between the cough jet and the PAC-generated air jet. From the case only with the background ventilation system (Fig. 2S), the cough jet at t = 0.8 s already reached the HP. Thus, the visualization at t = 0.8 s was selected to investigate the interaction between the cough jet and the PAC-generated flow around the HP under various scenarios.

When the PAC generated an upward velocity of 3 m/s, the cough jet was slightly blown upward by the PAC-generated air jet at 15 cm from the HP. However, when the distance between the PAC and the HP was 40 and 65 cm, the PAC-generated air jet

bent the cough jet upward and deviated from the inhalation zone of the HP. The exposure reduction varied from 42% ± 9% to 61% ± 4% when the flow rate of the PAC was 9 L/s, as shown in Fig. 7. The exposure reduction was the lowest (42%) at 40 cm and highest (61%) at 15 cm, different from the visualization of the scenarios of PAC/9-D15, PAC/9-D40 and PAC/9-D65 in Fig. 6. The possible reason was that, though the cough jet was deviated from the inhalation zone by the PAC flow, cough droplets did not move far away from the HP and were still around the HP due to low velocity (3 m/s) of the PAC. Hence, the combined effect of the PAC flow, thermal plume, and the background ventilation system resulted in different dispersion of cough droplets around the HP.

When the PAC velocity increased to 5, 7, and 9 m/s, the cough jet was blocked by the PAC air jet with the PAC at 15 cm away from the HP (Fig. 6). Furthermore, when the distance between the PAC and the HP increased to 40 and 65 cm, the cough jet was blown upward. The upward angle of the cough jet was larger than that with the PAC velocity of 3 m/s. It was also found that when the distance between the PAC and the IP was closer, the cough jet from the IP was blocked earlier by the PAC airflow. Despite different visualization with PAC at different distances and velocities, the main feature was that the cough jet was blocked and/or blown upward by the PAC flow and did not reach the HP.

As shown in Fig. 7, the exposure reduction caused by PAC at velocities of 5, 7, and 9 m/s and different distances of 15, 40 and 65 cm from the HP was similar, ranging between 83% ± 2% and 87% ± 0.6%. When the PAC velocity increased to 5 m/s or more, the increase in velocity and the distance between the HP and the PAC had little effect on reducing exposure. The possible explanation was that the increased PAC velocity could diminish the horizontal movement of cough droplets and blow the

airborne droplets to the upper part of the indoor environment when the PAC was 40 and 65 cm away from the HP, and/or prevent the cough droplets from reaching the HP when the distance between PAC and HP was 15 cm. Under such circumstances, the dispersion of airborne droplets was mainly influenced by the background ventilation system.

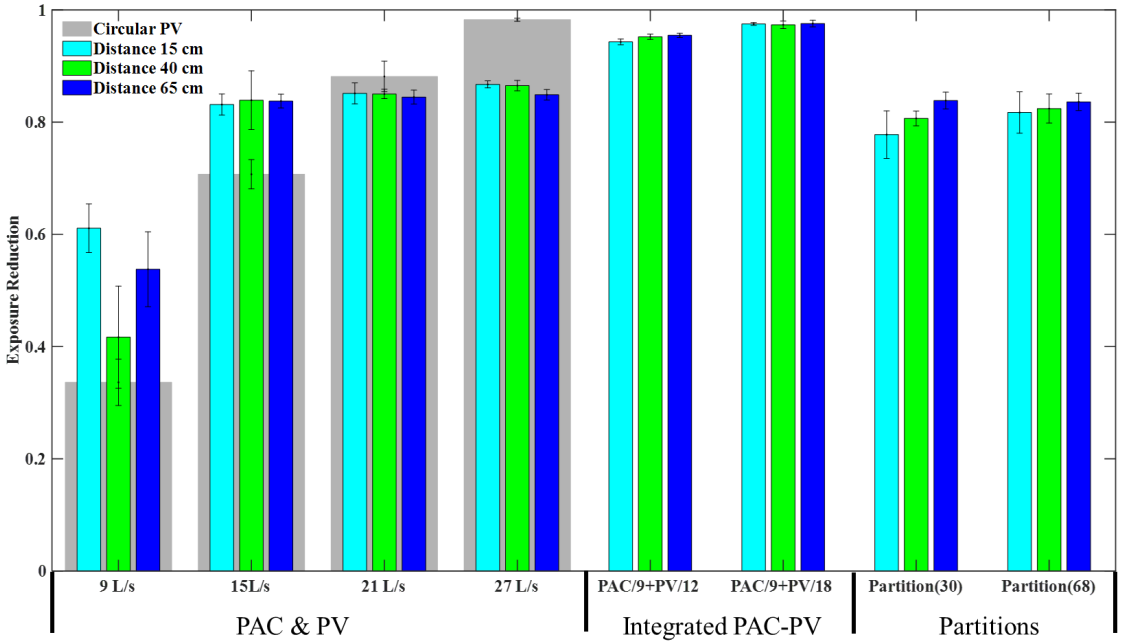

Figure 7 Exposure reduction of the HP influenced by PAC, PV, Integrated PAC-PV, and partitions. The mean and standard deviation (error bar) of exposure reduction are reported in each histogram. Note: In groups of PAC&PV, grey bars represent exposure reduction by PV, while cyan, green and blue bars mean exposure reduction by PAC at distances of 15, 40, and 65 cm from the HP, respectively. In groups of integrated PAC-PV, cyan, green and blue bars indicate exposure reduction by PAC-PV when the PAC was at distances of 15, 40, and 65 cm from the HP, respectively. In groups of partitions, cyan, green and blue bars denote exposure reduction by partitions at distances of 15, 40, and 65 cm from the HP, respectively.

3.2 Comparison in exposure reduction between PAC and PV

The performance of PAC and PV in reducing airborne droplets at the same flow rates was compared. As shown in Fig. 7, when the flow rate of the PV was 9 and 15 L/s, the exposure reduction caused by PV was 34% ± 4% and 71% ± 3%, respectively, lower than that by PAC, respectively. When the flow rate was 21 and 27 L/s, exposure reduction generated by PV was higher than that by PAC, respectively. In particular, the exposure reduction of PV was up to 98% when the flow rate was 27 L/s.

With the increase of flow rate, the reduction in exposure caused by PV increased. The velocity generated by PV in the inhalation zone increased from 0.9 m/s to 2.5 m/s when the flow rate elevated from 9 L/s to 27 L/s (Table 2). The increased flow rate brought more fresh air to the inhalation zone. Unlike the effect of PAC on the cough jet, PV mainly protected the HP's inhalation zone from the airborne droplets. As shown in Fig. 8, at 0.6 s and 0.8 s, the cough jet was prevented by the PV flow around the inhalation zone. Differently, at 1.0 s -1.4 s, the dispersion of the cough jet became wider, and the cone area of the cough jet became larger over time. Though the microenvironment of the HP's inhalation zone was still protected by PV, the cough jet was dispersed out of the inhalation zone.

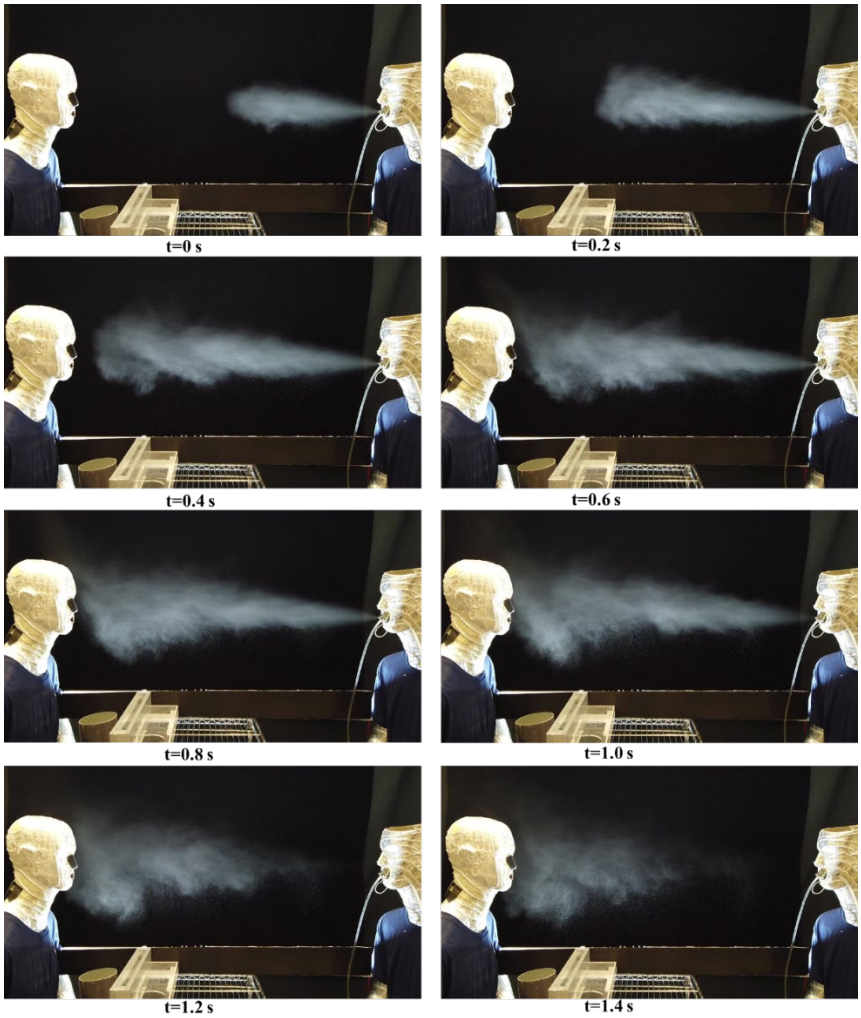

Figure 8 Visualization of interaction between cough jet and PV at a flow rate of 27 L/s

3.3 Performance of integrated PAC-PV

The performance of integrated PAC-PV on reducing exposure to airborne cough droplets was investigated. As shown in Fig. 7, exposure reduction for PAC/9+PV/12 and PAC/9+PV/18 was between 94% ± 0.5% and 98% ± 0.6%, which was higher than that of PAC (84% ± 1% - 87% ± 0.6%) alone at flow rates of 21 and 27 L/s. Fig. 9 shows the visualization of interaction between cough jet and integrated PAC/9-PV/18 with PAC at 15 cm from the HP. The cough jet was blown upward slightly and deviated from the inhalation zone, consistent with that of PAC at a flow rate of 9 L/s. However, the exposure reduction of the PAC-PV was much higher than that of PAC with the same

flow rate of 9 L/s (p <0.01). This was because after the PAC airflow blew the cough jet upward, the PV airflow further prevented the dispersed airborne droplets from entering the inhalation zone (Fig. 9 and Fig. 5S).

When the flow rate of PAC-PV increased from 21 L/s to 27 L/s, there was almost no increase in exposure reduction. Moreover, the exposure reduction of PAC-PV showed little relationship with the distance between the PAC and the HP, which was different from that of PAC with a flow rate of 9 L/s.

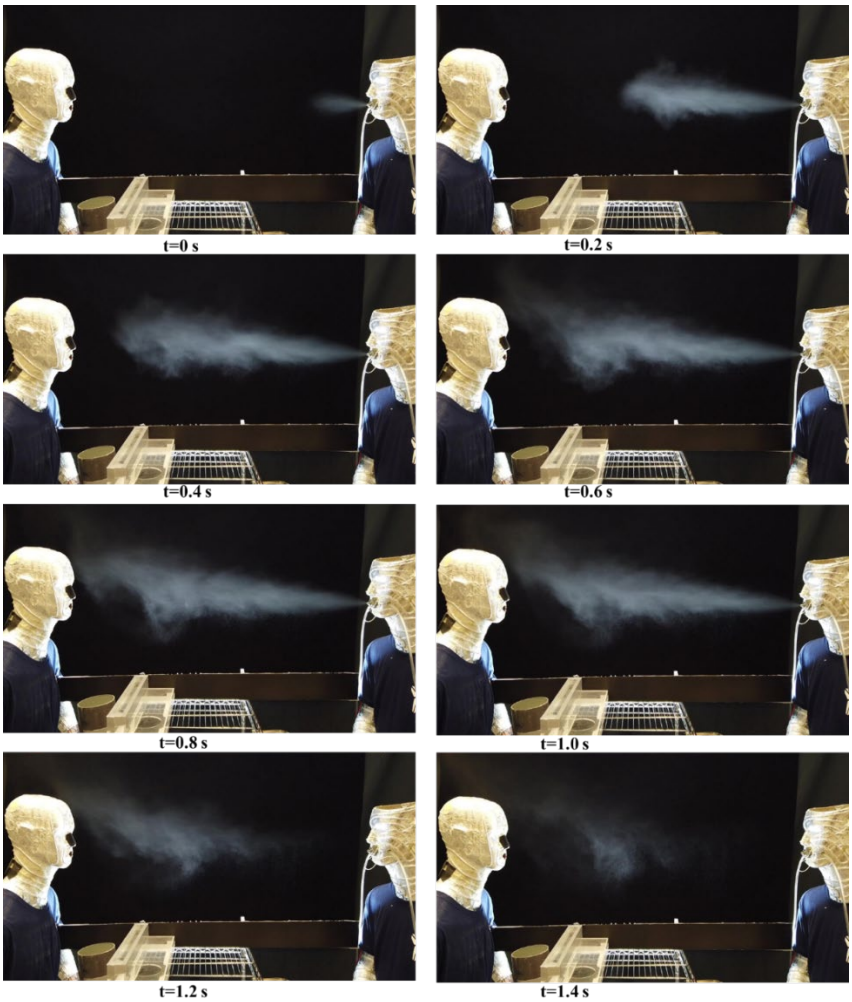

Figure 9 Visualization of interaction between the cough jet and integrated PAC/9-PV/18 with PAC at 15 cm from the HP

3.4 Performance of partitions

The exposure reduction of partitions with a width of 30 and 68 cm varied from 78% ± 4% to 84% ± 2% when the partition was 15 cm to 65 cm away from the HP (Fig. 7). The width of the partition did not affect the exposure reduction significantly. The highest exposure reduction caused by the partition was about 84% ± 2% when the partitions with a width of 30 and 68 cm was 65 cm away from the HP (Fig. 7). As shown in Fig. 7, the closer the partition to the IP, the better exposure reduction. The possible reason was that more cough droplets impinged and deposited on the partitions. A full-cone cough jet was released from the cough generator. When the IP was closer to the partition, the cone area of the cough jet was smaller and cough droplets concentrated in the small cone area with large momentum. Hence, more droplets would deposit on the partitions when the partition was closer to the IP.

Fig. 10 shows the visualization of interaction between the cough jet and the partition with a width of 30 cm. The cough jet hit the partition and then moved parallel along the surface of the partition. The partition effectively blocked the cough droplets that moved towards the HP, in line with the phenomenon reported by Wang et al. [37] who found that after hitting the front surface, the cough jet became a parallel diffuse flow, spreading upward and downward along the surface. Afterwards, the airborne droplet nuclei were dispersed in the indoor environments, mainly dominated by the background ventilation system and the thermal plume of the HP and IP.

By comparison, the exposure reduction caused by partitions was higher than that of PAC at a flow rate of 9 L/s, but similar to or lower than that of PAC with flow rates of 15, 21 and 27 L/s. In this work, we only investigated partitions with two different widths. More work on varied heights and widths of partitions is needed.

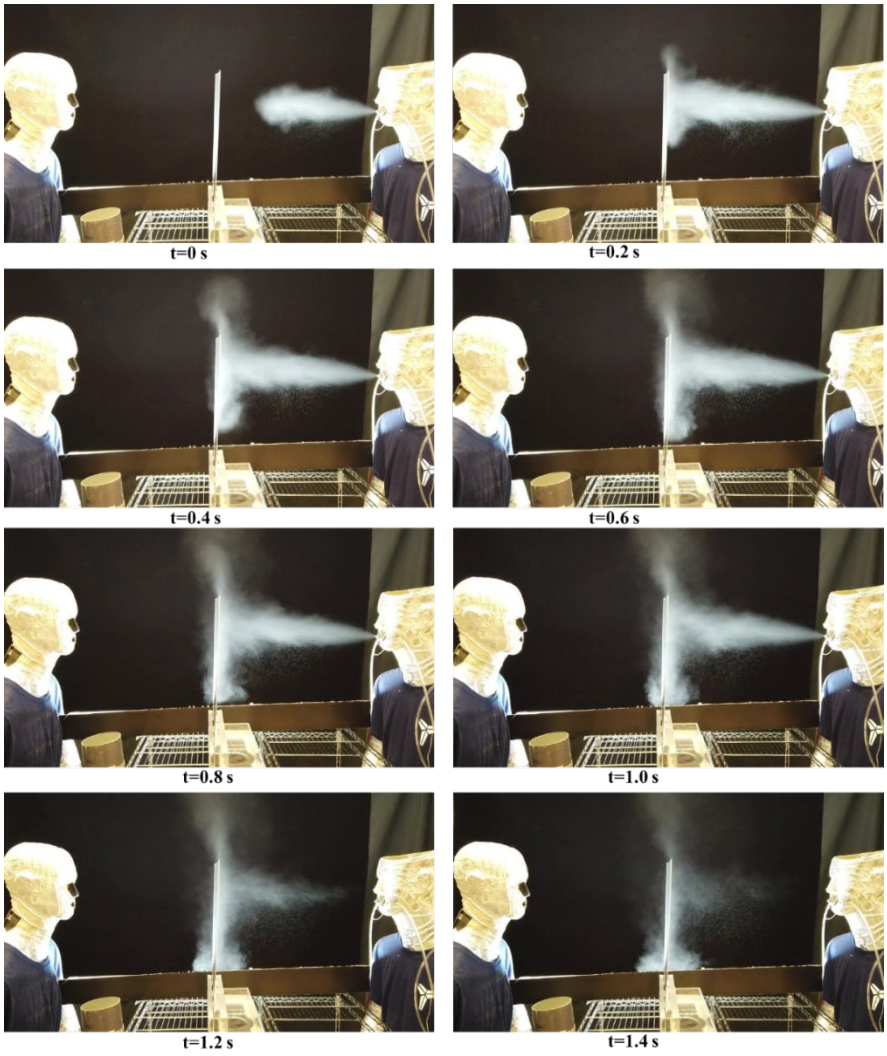

Figure 10 Visualization of interaction between a partition (with a width of 30 cm) and the cough jet when the partition is at 40 cm from the HP.

4 Discussion

The main goal of this study was to investigate whether the PAC was able to efficiently reduce the exposure of healthy people to airborne droplets released by an infected person in close contact. Our findings demonstrated that the PAC had a good performance in reducing exposure to airborne droplets.

The exposure reduction of PAC ranged from 42% to 87% depending on flow rate and distance between the HP and PAC. When the velocity increased to a ‘critical

velocity' and above, such as 5 m/s in this work, exposure reduction was almost stable (83% - 87%) and the distance between PAC and HP no longer had impact on the performance of PAC on reducing exposure to airborne droplets. The 'critical velocity' of PAC in this work suggests that once the 'critical velocity' is determined, high exposure reduction of PAC can be achieved and there is no need to further increase the flow rate which enhances energy consumption. In addition, the results indicate that people can adjust the position of PAC according to their preferences due to irrelevance between exposure reduction and distance from PAC to the HP.

Different from PAC, PV with an increased flow rate resulted in an increased exposure reduction. The performance of PV in this work was consistent with previous results reported by Xu et al. [23], who found that PV with a high flow rate could effectively protect the healthy person. In addition, other studies [20, 38] also indicated that increased flow rate of PV led to higher exposure reduction because more fresh air was sent to the inhalation zone.

Previous studies [21, 38, 39] mainly focused on the importance of PV on reducing the airborne cross-infection. In some cases, the application of PV could increase the exposure of the users due to entrainment of airflow [16, 23]. In addition, when PV was used by the IP, expiratory droplets may be more likely to be spread in enclosed environments, which resulted in a higher exposure for the healthy person [18]. Different from the PV that usually sends fresh air to the inhalation zone, PAC blows the airflow vertically upward between the HP and IP (Fig. 1 (c)). For the situation investigated in this work, no matter who was the IP, which is the cough jet released from the people in the left or right side in Fig. 1. The vertical PAC flow between these two people could block the incoming cough jet or change the motion direction of the cough jet to avoid the direct exposure of the other one.

The high air velocity (2.0 and 2.5 m/s) around the HP's face caused by PV in this work possibly resulted in draught risk or eye irritation. Differently, PAC airflow was blown upward vertically. The air velocity around the HP and IP was almost unchanged. PAC would not likely affect the thermal comfort and result in draught risk or eye irritation for the users. In order to better understand PAC and PV systematically, the comparison of the performance of PAC and PV in draught risk and thermal comfort is needed in the future work by considering main factors such as room temperature and clothing.

Strikingly, exposure reduction caused by the integrated PAC-PV was more significant. The reduction in exposure reached 94% - 98%, much better than that of PAC alone. This was due to the fact that the PAC in the integrated PAC-PV system changed the motion direction of cough jet and deviated it from the HP's inhalation zone, while the PV sent the fresh air to the inhalation zone, which further reduced the exposure of the HP to airborne droplets. More studies are necessary to investigate the performance of the integrated PAC-PV system in reducing exposure to airborne droplets when PAC has different flow rates in the system.

By comparing partitions, PAC, and PAC-PV, exposure reduction caused by PAC-PV was much higher than that of PAC and partitions in this work. The exposure reduction caused by PAC in this work could be higher than that of partitions when the flow rates generated by PAC were high enough since the PAC not only blocked the cough jet, but also blew the cough jet upward. The highest exposure reduction (84%) by partitions was almost the same as that of PAC at a flow rate of 15 L/s. Energy consumption was calculated for further consideration in this work. Fig. 11 presents the comparison of the annual energy costs (C) between PAC, PV, PAC-PV, and partitions, which does not consider the maintenance fee and installation fee. C was calculated

using equation (S1) as shown in supporting information. The annual fee for PAC, PV and PAC-PV is within eight dollars. When maintaining the exposure reduction of 84%, the annual fee consumed by the partitions is the lowest (zero) while the annual fee of PAC (PAC/15) is four dollars. The annual fee for the PAC-PV which has outstanding performance is only between five and seven dollars.

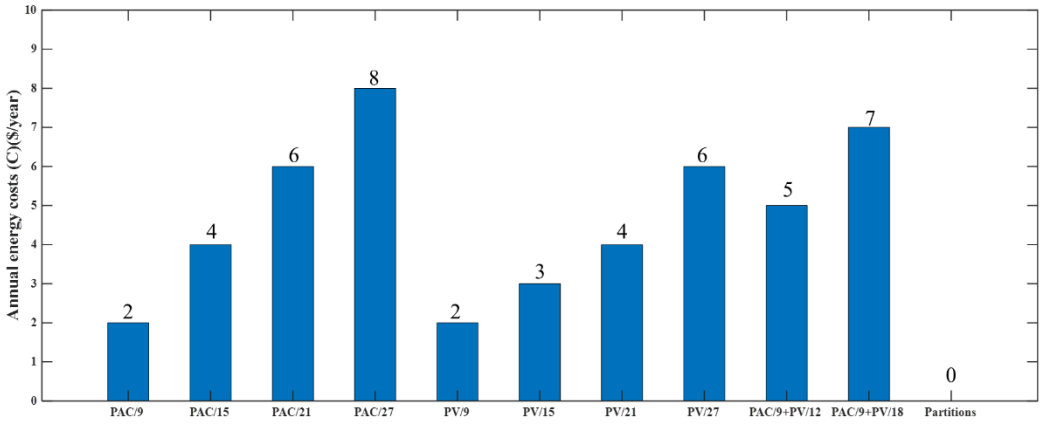

Figure 11 The annual energy costs of PAC, PV, PAC-PV, and partitions

The above analysis suggests that in addition to PV tested in previous studies and partitions widely used nowadays due to COVID-19, PAC and the integrated PAC-PV can be alternative methods to reduce the short-range airborne transmission. These two systems can be installed in densely populated offices, airplanes, buses, hospitals, and trains as mitigation measures to prevent the spread of respiratory diseases. Though face masks are worn today due to Covid-19, PAC and PAC-PV in this work can also be potential strategies supplementing face mask to reduce the exposure to airborne droplets. When the period of Covid-19 ends, people may not like to wear face masks in their daily life due to dyspnoea [40], thermal discomfort, and increased skin temperature [41]. However, people still need to face the risk of contrasting some other respiratory diseases, such as influenza. Thus, PAC and/or PAC-PV can be still used to protect the healthy people in the future.

Some limitations are identified in this work. Firstly, measurements were performed in the steady-state conditions, while real conditions could be much more complex due to people's movement and/or people's different head orientations. Secondly, this work only investigated the performance of PAC terminal with a fixed size. PAC with different width or length possibly has different performances in removing airborne droplets. Thirdly, this work focused on the expiratory droplets from cough activities which usually have large initial velocities. Expiratory droplets generated from talking and breathing with low initial velocities are also important sources for respiratory disease transmission. More studies are needed to investigate the performance of PAC in reducing exposure to airborne droplets from talking and breathing. Lastly, the current study focused on the performance of PAC on minimizing the inhalation of airborne droplets. No experiments have been done on the effectiveness of PAC on reducing the deposition of expiratory droplets on the HP and the dispersion of expiratory droplets in the indoor environment influenced by PAC. Further work is highly recommended.

5 Conclusions

This work investigated the performance of PAC in reducing exposure to cough droplets in close contact with an infected person. Simultaneously, the effectiveness of PAC was compared with that of PV, integrated PAC-PV, and partitions. The main conclusions of this study are summarized:

- Depending on the flow rate of PAC and distance between PAC and HP, the exposure reduction of PAC was from 42% to 87%. When the PAC velocity increased to a 'critical velocity', *e.g.,* 5 m/s, in this work, the exposure reduction remained high (83% - 87%) and almost stable. In addition, when PAC was at velocities of 5, 7, and 9 m/s, the distance between PAC and the HP almost had

no influence on the exposure reduction.

- Compared to PV, PAC had better exposure reduction when the flow rate was 9 and 15 L/s. However, when the flow rate was increased to 21 and 27 L/s, the exposure reduction of PV was higher than that of PAC. Since the velocity in the inhalation zone caused by PV was about 2.0 and 2.5 m/s when the flow rate was 21 and 27 L/s, respectively, the high velocity around the face possibly resulted in draught risk and eye irritation.
- The exposure reduction of integrated PAC-PV was between 94% and 98%, indicating that the PAC-PV had outstanding performance in reducing airborne droplets.
- In comparison, the exposure reduction caused by PAC was slightly higher than that of partitions.
- PAC and the integrated PAC-PV can be alternative methods, apart from PV and partitions, to reduce the exposure to airborne droplets caused by cough activities during close contact.

Acknowledgement

This work was supported by the University Strategic Importance scheme (1-ZE1M); the Strategic Focus Area scheme of The Research Institute for Sustainable Urban Development (1-BBW9) and the University Postdoctoral Fellowship Scheme (W14L) of The Hong Kong Polytechnic University; and the Research Grants Council of the Hong Kong Special Administrative Region via Theme-Based Research Scheme (TRS) (Project T24-504/17-N). The authors thank the Hong Kong University of Science and Technology for providing experimental facilities. Thanks also go to Haoxian Lu, Kaimin Li, and Dawen Yao for their help in the experimental setup.

References

[1] S. Stelzer-Braid, B.G. Oliver, A.J. Blazey, E. Argent, T.P. Newsome, W.D. Rawlinson, E.R. Tovey, Exhalation of respiratory viruses by breathing, coughing, and talking, J. Med. Virol. 81(9) (2009) 1674-1679.

[2] D.K. Milton, M.P. Fabian, B.J. Cowling, M.L. Grantham, J.J. McDevitt, Influenza virus aerosols in human exhaled breath: particle size, culturability, and effect of surgical masks, PLoS Pathog. 9(3) (2013) e1003205.

[3] W.G. Lindsley, F.M. Blachere, R.E. Thewlis, A. Vishnu, K.A. Davis, G. Cao, J.E. Palmer, K.E. Clark, M.A. Fisher, R. Khakoo, Measurements of airborne influenza virus in aerosol particles from human coughs, PloS One 5(11) (2010) e15100.

[4] Y. Li, G.M. Leung, J.W. Tang, X. Yang, C.Y. Chao, J.Z. Lin, J.W. Lu, P.V. Nielsen, J. Niu, H. Qian, A.C. Sleigh, H.J. Su, J. Sundell, T.W. Wong, P.L. Yuen, Role of ventilation in airborne transmission of infectious agents in the built environment - a multidisciplinary systematic review, Indoor Air 17(1) (2007) 2-18.

[5] Z. Ai, A.K. Melikov, Airborne spread of expiratory droplet nuclei between the occupants of indoor environments: a review, Indoor Air 28(4) (2018) 500-524.

[6] J. Wei, Y. Li, Airborne spread of infectious agents in the indoor environment, Am. J. Infect. Control 44(9) (2016) S102-S108.

[7] P.V. Nielsen, Control of airborne infectious diseases in ventilated spaces, J. R. Soc. Interface 6 Suppl 6 (2009) S747-55.

[8] H. Qian, Y. Li, P.V. Nielsen, C.-E. Hyldgård, T.W. Wong, A. Chwang, Dispersion of exhaled droplet nuclei in a two-bed hospital ward with three different ventilation systems, Indoor Air 16(2) (2006) 111-128.

[9] P.V. Nielsen, Y. Li, M. Buus, F.V. Winther, Risk of cross-infection in a hospital ward with downward ventilation, Build. Environ. 45(9) (2010) 2008-2014.

[10] M.J. Mendell, E.A. Eliseeva, M.M. Davies, M. Spears, A. Lobscheid, W.J. Fisk, M.G. Apte, Association of classroom ventilation with reduced illness absence: a prospective study in C alifornia elementary schools, Indoor Air 23(6) (2013) 515-528.

[11] Z.D. Bolashikov, A.K. Melikov, W. Kierat, Z. Popiołek, M. Brand, Exposure of health care workers and occupants to coughed airborne pathogens in a double-bed hospital patient room with overhead mixing ventilation, HVAC&R Res. 18(4) (2012) 602-615.

[12] J. Pantelic, K.W. Tham, Adequacy of air change rate as the sole indicator of an air distribution system's effectiveness to mitigate airborne infectious disease transmission caused by a cough release in the room with overhead mixing ventilation: a case study, HVAC&R Res. 19(8) (2013) 947-961.

[13] A. Lipczynska, J. Kaczmarczyk, A.K. Melikov, Thermal environment and air quality in office with personalized ventilation combined with chilled ceiling, Build. Environ. 92 (2015) 603-614.

[14] Z.J. Zhai, I.D. Metzger, Insights on critical parameters and conditions for personalized ventilation, Sustain. Cities Soc. 48 (2019) 101584.

[15] J. Liu, S. Zhu, M.K. Kim, J. Srebric, A Review of CFD Analysis Methods for Personalized Ventilation (PV) in Indoor Built Environments, Sustainability 11(15) (2019) 4166.

[16] J. Xu, S. Fu, C.Y. Chao, Performance of airflow distance from personalized ventilation on personal exposure to airborne droplets from different orientations, Indoor Built Environ. (2020) 1420326X20951245.

[17] J. Xu, C. Wang, S. Fu, K. Chan, C.Y. Chao, Short-range Bioaerosol Deposition and Inhalation of Cough Droplets and Performance of Personalized Ventilation, Aerosol Sci. Tech. 55(4) (2021) 474-485.

[18] X. Li, J. Niu, N. Gao, Co-occupant's exposure to exhaled pollutants with two types of personalized ventilation strategies under mixing and displacement ventilation systems, Indoor Air 23(2) (2013) 162-171.

[19] C. Shen, N. Gao, T. Wang, CFD study on the transmission of indoor pollutants under personalized ventilation, Build. Environ. 63 (2013) 69-78.

[20] J. Yang, S. Sekhar, K. Cheong, B. Raphael, Performance evaluation of a novel personalized ventilation–personalized exhaust system for airborne infection control, Indoor Air 25(2) (2015) 176-187.

[21] J. Pantelic, K.W. Tham, D. Licina, Effectiveness of a personalized ventilation system in reducing personal exposure against directly released simulated cough droplets, Indoor Air 25(6) (2015) 683-93.

[22] J. Pantelic, G.N. Sze-To, K.W. Tham, C.Y. Chao, Y.C. Khoo, Personalized ventilation as a control measure for airborne transmissible disease spread, J. R. Soc. Interface 6 Suppl 6 (2009) S715-26.

[23] C. Xu, X. Wei, L. Liu, L. Su, W. Liu, Y. Wang, P.V. Nielsen, Effects of personalized ventilation interventions on airborne infection risk and transmission between occupants, Build. Environ. (2020) 107008.

[24] R. Cermak, A.K. Melikov, Protection of occupants from exhaled infectious agents and floor material emissions in rooms with personalized and underfloor ventilation, HVAC&R Res. 13(1) (2007) 23-38.

[25] G. Cao, K. Sirén, S. Kilpeläinen, Modelling and experimental study of performance of the protected occupied zone ventilation, Energy Build. 68 (2014) 515-531.

[26] G. Cao, P. Nielsen, R. Jensen, P. Heiselberg, L. Liu, J. Heikkinen, Protected zone ventilation and reduced personal exposure to airborne cross-infection, Indoor Air 25(3)

(2015) 307-319.

[27] A. Aganovic, G. Cao, Evaluation of airborne contaminant exposure in a single-bed isolation ward equipped with a protected occupied zone ventilation system, Indoor Built Environ. 28(8) (2019) 1092-1103.

[28] A. Aganovic, M. Steffensen, G. Cao, CFD study of the air distribution and occupant draught sensation in a patient ward equipped with protected zone ventilation, Build. Environ. 162 (2019) 106279.

[29] A. Handbook, ASHRAE handbook–fundamentals, Atlanta, GA (2009).

[30] G. Sze To, M. Wan, C. Chao, L. Fang, A. Melikov, Experimental study of dispersion and deposition of expiratory aerosols in aircraft cabins and impact on infectious disease transmission, Aerosol Sci. Tech. 43(5) (2009) 466-485.

[31] A.K. Melikov, Personalized ventilation, Indoor Air 14 (2004) 157-167.

[32] A.K. Melikov, R. Cermak, M. Majer, Personalized ventilation: evaluation of different air terminal devices, Energy Build. 34(8) (2002) 829-836.

[33] D. Al Assaad, K. Ghali, N. Ghaddar, E. Katramiz, S. Ghani, Evaluation of different personalized ventilation air terminal devices: Inhalation vs. clothing-mediated exposures, Build. Environ. 192 (2021) 107637.

[34] C. J. Chen, W. Rodi,Vertical turbulent buoyant jets: a review of experimental data, NASA STI/Recon Technical Report A 80 (1980) 23073.

[35] I. Kulmala, P. Hynynen, I. Welling, A. Säämänen, Local ventilation solution for large, warm emission sources, Ann. Occup. Hyg. 51 (2007) 35-43.

[36] J. Wei, Y. Li, Enhanced spread of expiratory droplets by turbulence in a cough jet, Build. Environ.93 (2015) 86-96.

[37] C.T. Wang, S.C. Fu, C.Y.H. Chao, Short-range bioaerosol deposition and recovery of viable viruses and bacteria on surfaces from a cough and implications for respiratory

disease transmission, Aerosol Sci. Tech. 55(2) (2021) 215-230.

[38] H. Alsaad, C. Voelker, Could the ductless personalized ventilation be an alternative to the regular ducted personalized ventilation?, Indoor Air 31 (2020) 99-111.

[39] C. Xu, P.V. Nielsen, L. Liu, R.L. Jensen, G. Gong, Impacts of airflow interactions with thermal boundary layer on performance of personalized ventilation, Build. Environ. 135 (2018) 31-41.

[40] L. Serresse, N. Simon-Tillaux, M. Decavèle, F. Gay, N. Nion, S. Lavault, A. Guerder, A. Châtelet, F. Dabi, A. Demoule, Lifting dyspnoea invisibility: COVID-19 face masks, the experience of breathing discomfort, and improved lung health perception—a French nationwide survey, Eur. Respir. J. (2021).

[41] A. Scarano, F. Inchingolo, F. Lorusso, Facial skin temperature and discomfort when wearing protective face masks: thermal infrared imaging evaluation and hands moving the mask. Int. J. Environ. Res. Public Health 17 (2020) 4624.